Tracking Radical Migration in Large Hydrogen Deficient Peptides with Covalent Labels: Facile Movement does not Equal Indiscriminate Fragmentation

Tony Ly and Ryan R. Julian
Department of Chemistry, University of California, Riverside, California, USA

Photodissociation of iodo-tyrosine modified peptides yields localized radicals on the tyrosine side chain, which can be further dissociated by collisional activation. We have performed extensive experiments on model peptides, RGYALG, RGYG, and their derivatives, to elucidate the mechanisms underlying backbone fragmentation at tyrosine. Neither acetylation nor deuteration of the tyrosyl phenolic hydrogen significantly affects backbone fragmentation. However, deuterium migration from the tyrosyl β carbon is concomitant with cleavage at tyrosine. Substitution of tyrosine with 4-hydroxyphenylglycine, which does not have β hydrogens, results in almost complete elimination of backbone fragmentation at tyrosine. These results suggest that a radical situated on the β carbon is required for a-type fragmentation in hydrogen-deficient radical peptides. Replacement of the αH of the residue adjacent to tyrosine with methyl groups results in significant diminution of backbone fragmentation. The initial radical abstracts an αH from the adjacent amino acid, which is poised to "rebound" and abstract the βH of tyrosine through a six-membered transition-state. Subsequent β-scission leads to the observed a-type backbone fragment. These results from deuterated peptides clearly reveal that radical migration in peptides can occur and that multiple migrations are not infrequent. Counterintuitively, close examination of all experimental results reveals that the probability for fragmentation at a particular residue is well correlated with thermodynamic radical stability. A-type fragmentation therefore appears to be most likely when favorable thermodynamics are combined with the relevant kinetic control. These results are consistent with ab initio calculations, which demonstrate that barriers to migration are significantly smaller in magnitude than probable dissociation thresholds. (J Am Soc Mass Spectrom 2009, 20, 1148–1158) © 2009 American Society for Mass Spectrometry

Odd electron species play important roles in living systems. One of the specific functions of these reactive species is to assist enzymatic catalysis of biologically important redox reactions [1]. In addition to their relevance to biochemistry, protein radicals are of significant interest in mass spectrometry. This is largely due to the development and successful application of radical-based dissociation techniques. Both electron capture dissociation (ECD) and electron transfer dissociation (ETD) are now conventional methods in proteomic analyses [2, 3]. The mechanisms governing dissociation for both techniques are still under investigation [4]. It has been suggested that capture of a single electron leads to a single backbone cleavage [5, 6]. Surprisingly however, ECD of a cyclic peptide yields observable fragmentation after capture of a single electron, which can only occur if the backbone is cleaved at multiple sites. O'Connor and coworkers have proposed that hydrogen-deficient z· fragments produced by ECD further dissociate through a series of cascading reactions [7]. This hypothesis is also corroborated by results from other experiments where covalent attachment of radical trap moieties reduces the sequence coverage observed in ECD experiments and by evidence that extensive hydrogen atom migration occurs after electron capture [8–10]. More recently, ECD of solvated peptides shows that c and z· formation is correlated with the ability of the solvent to "cage" a hydrogen atom [11]. These results suggest that radical chemistry may play a significant role in the fundamental dissociation mechanisms of ECD. Other radical-based dissociation methods have also been developed to interrogate peptides and proteins. In these experiments, specific bonds are modified either covalently, [12–14] or by attachment of a metal-complex, [15–17] such that the bond is predisposed towards homolytic cleavage. Activation of these precursor molecules by CID generates the radical species.

Photodissociation (PD) is an alternative method for generating radicals by electronic excitation of a suitable

Address reprint requests to Dr. R. R. Julian, Department of Chemistry, University of California, Riverside, CA 92521, USA. E-mail: ryan.julian@ucr.edu

1044-0305/09/$32.00
doi:10.1016/j.jasms.2009.02.009

Published online February 12, 2009
Received September 12, 2008
Revised January 29, 2009
Accepted February 5, 2009

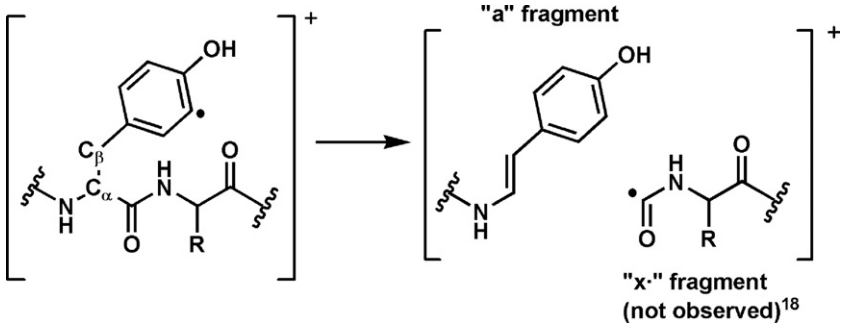

Scheme 1

precursor [18]. Undesirable side reactions are avoided with PD due to the specificity of the excitation chemistry. PD can be coupled with noncovalent or covalent delivery of the photolabile group, and a variety of precursor chemistries have been identified [19–21]. Of particular interest for the present work, we have previously demonstrated that PD of iodine-labeled proteins with 266 nm photons results in selective homolytic dissociation of the carbon-iodine bond to regiospecifically generate a radical on the side-chain of tyrosine in high yield. Subsequent collisional activation of these radical proteins yields a-type backbone fragmentation at the modified tyrosine. Scheme **1** shows the reactant radical species and the backbone fragmentation products.

The observed selectivity favoring fragmentation at tyrosine is puzzling for two reasons. First, the initial radical is expected to be highly reactive. To explain, comparison of relative C–H bond dissociation energies (BDEs) can be used to estimate the reactivity of the initial radical. The C–H BDE of benzene, which should be similar to the tyrosyl radical, is 472 ± 2 kJ/mol [22]. Typical C–H BDEs in the remaining peptide are much lower. For example, the αC–H BDEs have been calculated to be in the range of 316–369 kJ/mol [23]. Thus, abstraction of a hydrogen atom by the initial tyrosyl radical will be exothermic for all non aromatic hydrogens, in some cases by a significant amount. Therefore, radical migration away from tyrosine should be nonselective and facile, absent any significant barriers to migration. The second reason that the observed selectivity is not expected is because the radical is separated from the scissile site by four bonds, and cannot generate the observed products directly. Furthermore, electronic rearrangement is unlikely due to the localization of the radical in a σ orbital [24]. This fact, along with the steric constraints imposed by the rigid tyrosine side-chain, suggests that radical rearrangement or migration must occur before dissociation.

The present work focuses on a small group of peptides and their deuterated derivatives to examine the mechanism for selective fragmentation at tyrosine. Covalent labeling experiments reveal that the β hydrogen of tyrosine and the α hydrogen from either adjacent amino acid are involved in backbone fragmentation at tyrosine. We propose a "rebound" mechanism to account for these results. The initial tyrosyl radical abstracts a hydrogen atom from the α-carbon of an adjacent residue. This α-radical then "rebounds" and abstracts the hydrogen from the β-carbon of tyrosine due to a favorable six-membered transition-state. Subsequent β-scission leads to the observed backbone fragmentation. Results from deuterated peptides also indicate that radical migration and multiple migrations can occur. Interestingly, it is observed that radicals are most likely to initiate backbone fragmentation from thermodynamically favored β-positions with the most radical stabilization (as can be quantified by the lowest C–H BDE). Theoretical calculations suggest that this apparent combination of kinetic and thermodynamic control results from the facile migration of radicals, which is constrained by barriers that are substantially below dissociation thresholds.

Materials and Methods

All reagents were used as received unless specified. Diethyl ether, ethyl acetate, dichloromethane, absolute ethanol, LC-MS grade acetonitrile, methanol, chloramine-T, sodium metabisulfite, sodium chloride, sodium sulfate (anhydrous), sodium iodide, and sodium bicarbonate were purchased from Thermo-Fisher Scientific (Waltham, MA). Dimethylformamide (DMF), hexanes, fluorenylmethyloxycarbonyl (FMOC)-protected α-aminoisobutyric acid (AIB), acetyl anhydride, and acetic acid were purchased from EMD Biosciences (Gibbstown, NJ). Pyridine, benzotriazol-1-yl-oxytripyrrolidinophosphonium hexafluorophosphate (PyBOP), ninhydrin, 2,6-dichlorobenzoyl chloride (DCB), (D)-4-hydroxyphenylglycine and diisopropylethylamine (DIPEA) were purchased from Acros Organics (Morris Plains, NJ). α-d_2-Glycine was purchased from CDN Isotopes (Pointe-Claire, Quebec, Canada), while β-d_2-Tyrosine was purchased from Cambridge Isotope Laboratories (Andover, MA). FMOC-protected glycine, arginine(Pbf), leucine, and tyrosine(tBu) were purchased from LC Sciences (Houston, TX). FMOC-protected alanine, d_4-methanol (99.8%), D_2O (99.9%) and tri-isopropylsilane (TIS) were purchased from Sigma-Aldrich/Fluka (St. Louis, MO). Petroleum ether (Mallinckrodt-Baker, Phillipsburg, NJ), piperidine (Anaspec, San Jose, Ca), FMOC-O-succinimide

(FmocOSu) (ChemPep, Miami, FL), 1-hydroxybenzotriazole monohydrate (1-HOBt) (Chem Impex-International, Wood Dale, IL) were purchased. Aluminum-backed thin-layer chromatography (TLC) plates were purchased from Sorbent Technologies (Atlanta, GA). RGYALG, RPPGYSPFR, and RPPGFSPYR peptides were purchased from American Peptide Company (Sunnyvale, CA).

Free amino acids were protected with FmocOSu according to published procedures [25, 26]. Briefly, 1 equivalents of FmocOSu was added to 1 equivalents of $NaHCO_3$ and 1 equivalents of amino acid in water/acetone. The reaction mixture was stirred for 24 h, after which the absence of a free amino group was checked by TLC-ninhydrin analysis. Peptides were synthesized manually using Fmoc chemistry on a Wang resin (Acros Organics) [27]. The DCB method was used to load the first residue onto the resin. Subsequent chain extension reactions were achieved using PyBOP activation. Peptides were cleaved from the solid support using a solution of 95:2.5:2.5 TFA:H_2O:TIS for 2 h, after which the solvent was evaporated. The white peptide film was carefully washed with cold diethyl ether, redissolved in water, and lyophilized.

Peptides were iodinated using a published protocol [19]. In a typical iodination reaction, 1 equivalents of chloramine-T was added to a 50–100 μL solution containing 1 equivalents of peptide (~1–50 nmol) and 1 equivalents of sodium iodide. After 30 s, the reaction was quenched by adding 2 equivalents of sodium metabisulfite. Peptide acetylation was accomplished by adding 20 μL of acetic anhydride to 5 nmol of iodinated peptide dissolved in 100 mM ammonium acetate buffer. After a 10 min reaction time, the mixture was lyophilized. A separate aliquot of 5 nmol iodinated peptide was lyophilized and redissolved in 50/50 D_2O/CD_3OD to substitute all exchangeable hydrogens (i.e., attached to heteroatoms) with deuteriums.

Solutions containing 10 μM peptide in 50/50 water/acetonitrile were directly infused into a standard electrospray source of an LTQ linear ion trap mass spectrometer (Thermo-Fisher, Waltham, MA). Ions were collected in the linear ion trap, where mass spectrometry and dissociation experiments were performed. The electrospray needle voltage and capillary temperature were fixed at 5.0 kV and 215 °C, respectively. Voltages for the transfer optics were optimized to maximize the intensity of the singly protonated peak. A quartz window was installed on the back plate of the LTQ vacuum housing to transmit fourth-harmonic (266 nm) laser pulses from a flashlamp-pumped Nd:YAG "MiniLite" laser (Continuum, Santa Clara, CA) directly into the linear ion trap. Pulses were synchronized to the activation step of a typical MS^n experiment by feeding a TTL trigger signal from the mass spectrometer [28] to the laser via a digital delay generator (Berkeley Nucleonics, San Rafael, CA). Further MS^n experiments were performed by re-isolation and collision induced dissociation (CID) of the photodissociation (PD) product. We have found that the narrow isolation windows required to select the monoisotopic peak causes significant precursor ion heating. This leads to increased hydrogen/deuterium scrambling compared to when a wide isolation width is used. Therefore, the following experimental scheme was used for all peptides to minimize experimental artifacts arising from precursor ion heating. A 1.4 *m/z* isolation window was used to select the monoisotopic, singly protonated peak. A second isolation with a large window (10.0 *m/z*) was used to allow the ions to equilibrate to approximately room-temperature, [29], after which the laser was triggered. For the final step (MS^4), the radical peptide is re-isolated with a 10.0 *m/z* isolation window and collisionally activated. The default activation time (30.0 ms) was used for all MS^n steps.

Ab initio calculations were performed using the Gaussian 03 version 6.1 revision D.01 software suite (Gaussian, Inc., Wallingford, CT) using the hybrid density functional B3LYP and MPW1K methods with the 6-31++g(d,p) and 6-31+g(d,p) basis sets, respectively. Spin contamination was minimal for all systems. Candidate transition-state structures were found using the quasi-Newton synchronous transit (QST3) [30]. Frequency analyses at the same level of theory on all structures revealed no imaginary frequencies for minima and a single imaginary frequency for each transition-state structure. Visualization of the single imaginary frequency confirmed that the structure is indeed a saddle point connecting the reactants and products. Activation barriers are corrected for vibrational zero point energies, which are unscaled.

Results and Discussion

Figure 1a shows the PD spectrum for protonated iodo-RGYALG, $[RG^IYALG + H]^+$. The most abundant product is loss of iodine atom to yield a hydrogen deficient peptide radical. Hydrogen deficient is used in the context of a peptide missing a hydrogen relative to the mass of a fully protonated, even electron ion (with no implications about the specific structure of that ion) [31]. Due to the small size of this peptide internal conversion of residual energy from the laser pulse is sufficient to fragment some ions, resulting in the additional loss of isopropene from leucine (−56 Da). PD also produces a single backbone fragment in small abundance, the a_3 ion, which corresponds to cleavage of the C_α–C(O) bond of tyrosine. The yield of all radical product ions can be increased by re-isolating the peptide radical and performing further collisional activation, as shown in Figure 1b. In contrast to PD-CID of the iodopeptide, CID of the noniodinated peptide produces loss of ammonia and b ions [20]. Thus, the side-chain losses and a_3 ion are due to the unique chemistry afforded by the presence of the radical. Importantly, the selective fragmentation at tyrosine for this peptide resembles the backbone fragmentation at tyrosine residues observed for whole proteins [19]. Investigation of this smaller system should allow the details of fragmentation at tyrosine to be elucidated.

In addition to backbone fragmentation at tyrosine, side-chain fragmentation at leucine and tyrosine is

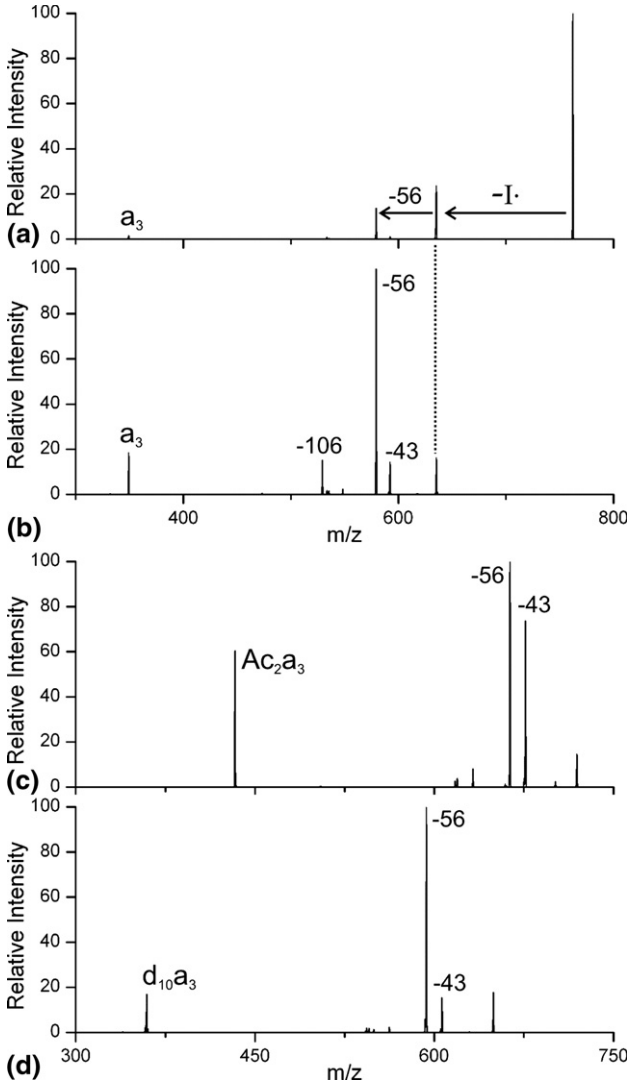

Figure 1. (**a**) Photodissociation of $[RG^{I}YALG + H]^+$ produces loss of I· as the most abundant product. (**b**) CID of [RGYALG· + H]$^+$ yields selective backbone fragmentation at the tyrosine residue (a_3). (**c**) CID of $[Ac_2RGYALG· + H]^+$. Acetylation of the tyrosine side-chain eliminates tyrosine side-chain loss. (**d**) CID of the fully deuterium-exchanged radical peptide, $[d_{14}RGYALG· + H]^+$ yields a kinetic isotope effect only for the loss of tyrosine side-chain. Thus, direct involvement of heteroatom hydrogens in backbone dissociation is unlikely.

observed in Figure 1b. Side-chain losses are commonly observed in radical-mediated peptide dissociation [12–21]. Most side-chain losses can be explained by hydrogen atom abstraction followed by β scission. A summary of the sites of hydrogen atom abstraction, the chemical formulae and the nominal masses of the observed side-chain fragments are given in Table 1.

Specific functional groups on the peptide, RGYALG, were covalently modified to determine whether these functionalities are essential to a_3 formation. The alcohol of the tyrosine side-chain was the first functionality tested. In theory, rearrangement of the radical within the tyrosine residue would yield the a_3 fragment [19]. Scheme 2 shows the details of this mechanism. The resonance-stabilized radical on the γ carbon of tyrosine can abstract the amide hydrogen to yield backbone fragmentation (bottom right). Alternatively, β scission produces loss of tyrosine side-chain (bottom left). To test this hypothesis, $RG^{I}YALG$ was acetylated at the N-terminus and the tyrosine OH. Figure 1c shows the PD-CID spectrum of the doubly acetylated peptide, $[Ac_2RGYALG· + H]^+$. The abundance of a_3 and -43 are increased, while the loss of tyrosine side-chain vanishes completely. This suggests that the proposed rearrangement does occur and is required for tyrosine side-chain loss, but is not strictly necessary to produce a_3.

To test whether any heteroatom hydrogens participate in this reaction, $RG^{I}YALG$ was dissolved in 50/50 D_2O/CD_3OD to exchange all labile hydrogen atoms for deuteriums. If formation of a_3 involves direct abstraction of an amide hydrogen, replacement with deuterium should incur a kinetic isotope effect. Figure 1d shows the PD-CID spectrum of the fully deuterated iodopeptide, $[d_{14}RGYALG· + H]^+$. Most ion abundances, including the a_3 ion, are similar to Figure 1b. The single major difference is the diminished intensity of tyrosine side-chain loss. This is most likely due to the replacement of the phenolic hydrogen with a deuterium, which results in a significant, attenuating kinetic isotope effect. This indicates that the phenolic hydrogen is required for tyrosine side-chain loss, which is consistent with the acetylation results mentioned above and mechanisms proposed in literature [15, 16]. In summary, these results suggest that formation of a_3 does not involve the phenolic or amide hydrogens of tyrosine or any other exchangeable hydrogens. Therefore, we must conclude that the dominant pathway yielding backbone fragmentation proceeds through a different mechanism than we originally proposed (Scheme 2) [19]. This implies, counterintuitively, that the tyrosyl radical must migrate to another residue and then preferentially return to tyrosine to yield the a_3 fragment.

This possibility can be explored by specifically replacing C–H bonds in the peptide with C–D bonds and then monitoring migration of deuterium, which should only occur by radical initiated chemistry. It should be noted that scrambling of carbon-deuterium bonds is not expected for closed-shell peptide ions [32, 33]. Substitution of hydrogen for deuterium in direct abstraction reactions typically results in significant kinetic isotope effects. Measured kinetic isotope effects for hydrogen abstraction by ·OH range from 2.0 to 6.8 and decrease linearly with temperature [34]. Thus, monitoring deu-

Table 1. Side chain fragmentation summary

Amino acid	Hydrogen abstracted	Nominal mass (Da)	Fragment
L	α	43	$CH_3CH·CH_3$
L	γ	56	$CH_2=C(CH_3)_2$
R	α	86	$CH_2CH_2NH(C=NH)NH_2$
R	γ	99	$CH_2=CHCH_2NH(C=NH)NH_2$
Y	ε	106	$CH_2=C_6H_4O$

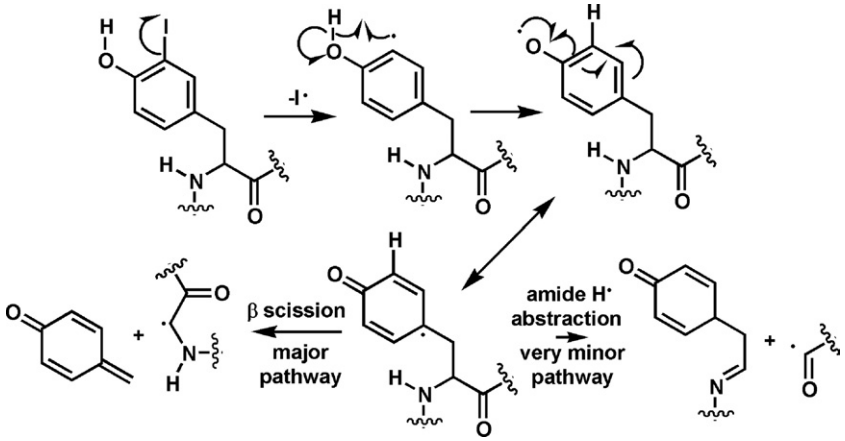

Scheme 2

terium transfers provides a lower limit to the extent of hydrogen transfers that would occur in an unlabeled peptide. Regardless of the magnitude, deuterium migration provides a record of where the radical has been, which can be used to elucidate radical-induced dissociation mechanisms in detail.

Abstraction of the β hydrogen from aromatic residues has been suspected to play a role in the fragmentation of radical peptides [14, 19]. The peptide $RGY_{\beta d2}ALG$ was synthesized to test whether the β hydrogens of tyrosine participate in the formation of a_3 ions. Figure 2a shows the CID spectrum of the resulting radical ion, $[RGY_{\beta d2}ALG\cdot + H]^+$. The a_3 fragment ion intensity is split between singly and doubly deuterated a_3. The simplest mechanism yielding d_1a_3 involves the migration of the initial radical to the ALG residues, which is followed by abstraction of one of the β deuteriums from tyrosine. The intensity of d_1a_3 is much greater than d_2a_3, which unequivocally shows that radical migration occurs before fragmentation of this peptide. Further CID of the even-electron d_2a_3 ion (shown in Figure 2b) also reveals radical migration. The relative intensities of d_1b_2, d_1a_2, and d_1b_1 indicate that ~90% of Gly2 has been deuterated. To summarize, migration of one of the β-deuteriums of tyrosine almost always precedes the formation of a_3, and can only occur following multiple radical migrations from the initial site.

The results in Figure 2a strongly suggest the β-hydrogens of tyrosine play a critical role in selective backbone dissociation. This hypothesis was investigated further by substituting 4-hydroxyphenylglycine (U) for tyrosine in the RGYALG peptide sequence. The side-chain of 4-hydroxyphenylglycine is a phenol attached directly to the α carbon of the peptide backbone and does not contain β hydrogens. The lack of β hydrogens to facilitate selective fragmentation should lead to the disappearance of the a_3 fragment. Figure 2c shows the CID spectrum for $[RGUALG\cdot + H]^+$. Backbone fragmentation almost completely disappears and side-chain loss at 4-hydroxyphenylglycine is absent. Interestingly, the a_3 fragment is observed at 0.2% relative abundance. This indicates that an alternative pathway exists to produce a_3, which does not involve the β hydrogens of tyrosine. This channel likely involves abstraction of the amide hydrogen, as proposed previously [19]. The intensity indicates that this is a very minor channel. By comparing the a_3 fragment intensities in Figure 2c and Figure 1b, we can conclude that the β hydrogen is essential for backbone fragmentation at tyrosine.

The results above illustrate how backbone fragmentation is preceded by radical migration to the β position of tyrosine. How does the initially generated radical arrive at the β carbon? The deuterium transfer demonstrated in Figure 2b (β carbon of Tyr3 to the α carbon of Gly2) suggests that the adjacent amino acid may facilitate radical transfer to the β carbon. To further evaluate whether the α-hydrogens of neighboring amino acids are essential to backbone fragmentation, we focused on a small tetrapeptide system. CID of $[RGYG\cdot + H]^+$ produces a_3 in good yield and loss of tyrosine side chain, as shown in Figure 3a, reproducing the selective cleavage at tyrosine. To examine the necessity of the α hydrogens of the glycine residues, experiments were next conducted with α-aminoisobutyric acid (designated with the single letter code J). This uncommon amino acid does not contain α hydrogens and prevents radical migration to the α carbon adjacent to tyrosine. Figure 3b shows the CID spectrum of $[RJYJ\cdot + H]^+$. The intensity of the a_3 ion in Figure 3b is significantly diminished relative to Figure 3a, which indicates that the α hydrogens of glycine in RGYG do facilitate backbone fragmentation at tyrosine. Even-electron counterparts of all other backbone fragments in Figure 3b (b_2, $b_3 + H_2O$, $c_1 - 2$) are found in the CID of the non-iodinated peptide (data not shown). The remaining a_3 ion intensity must be produced from another pathway. Radicals at other locations may also be able to abstract the β hydrogen of tyrosine. Indeed, abstraction of a hydrogen atom from the methyl groups of α-aminoisobutyric acid is feasible (the calculated BDE for the methyl group in alanine is 428 kJ/mol) [19]. However, the seven-membered transition-state for hydrogen

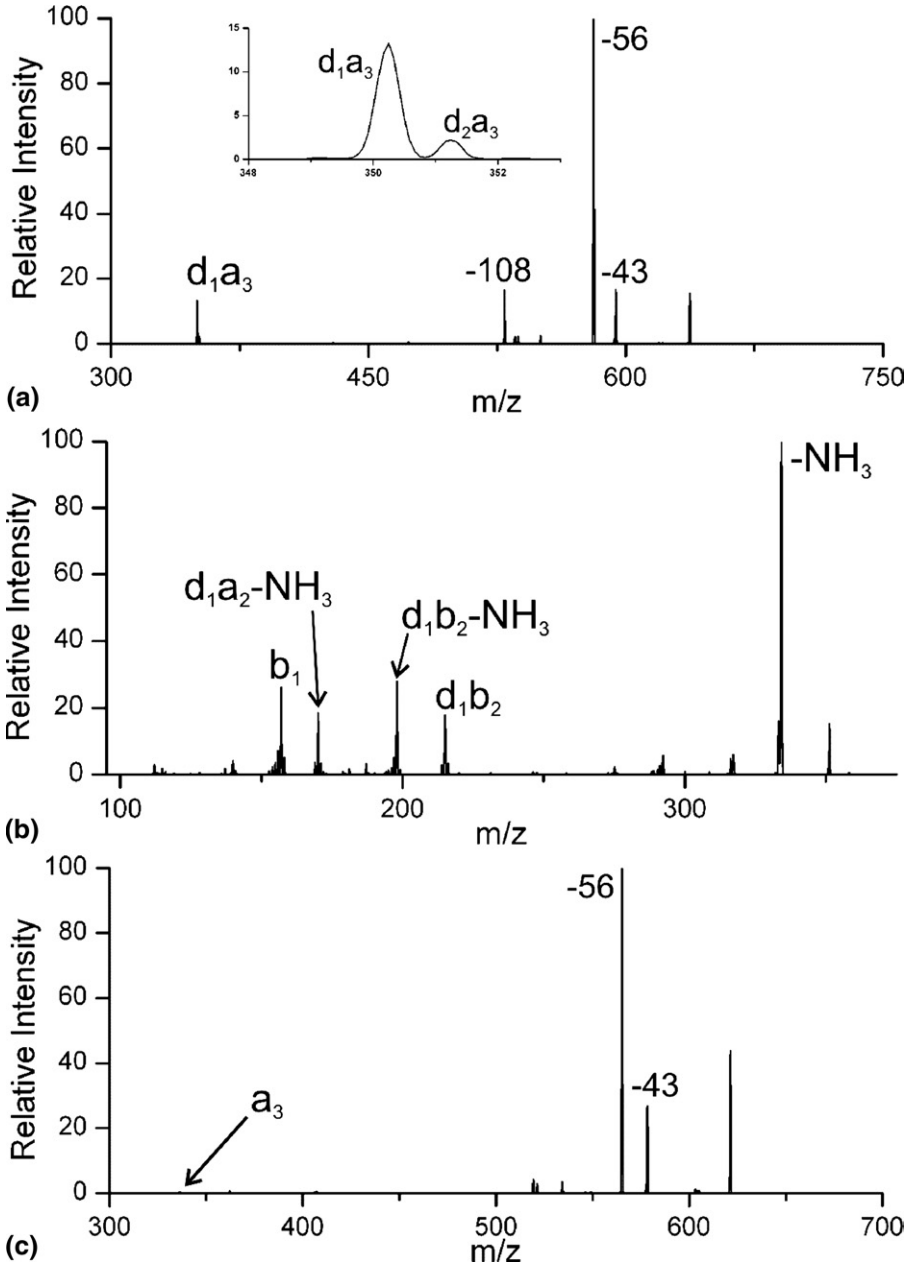

Figure 2. (**a**) CID of $[RGY_{d2}ALG\cdot + H]^+$. Examination of the a_3 fragment shows significant scrambling of the deuteriums, indicating that the β-hydrogens of tyrosine play a critical role in selective backbone dissociation. (**b**) Further CID of the doubly deuterated a_3 ion, $[d_2a_3 + H]^+$, from (**a**) shows that a deuterium has migrated to Gly2. (**c**) Replacement of tyrosine in RGYALG with 4-hydroxyphenylglycine, which has no β hydrogens results in almost complete elimination of selective fragmentation.

atom transfer from the methyl side chain of J to the β-position of tyrosine is not as favorable as for glycine. Transition states involving sites separated by a greater number of bonds are also possible, e.g., the initial radical site and the side chain of arginine. Regardless, the α-positions of the neighboring amino acid are shown to play an influential role in backbone fragmentation in this peptide model.

We propose the following "rebound" mechanism as the primary pathway yielding backbone fragmentation at tyrosine residues where the radical originates, as shown in Scheme 3. The initial radical abstracts a hydrogen atom from the α carbon of the adjacent amino acid. This captodatively-stabilized radical can then abstract the β-hydrogen from tyrosine through a kinetically favorable six-membered transition-state. Comparison of the calculated C–H BDEs for glycine (350 kJ/mol) and the β-hydrogens of tyrosine (367 kJ/mol) reveals that this abstraction is energetically feasible (ΔBDE = 17 kJ/mol) [20, 23]. This mechanism may access either the C- or

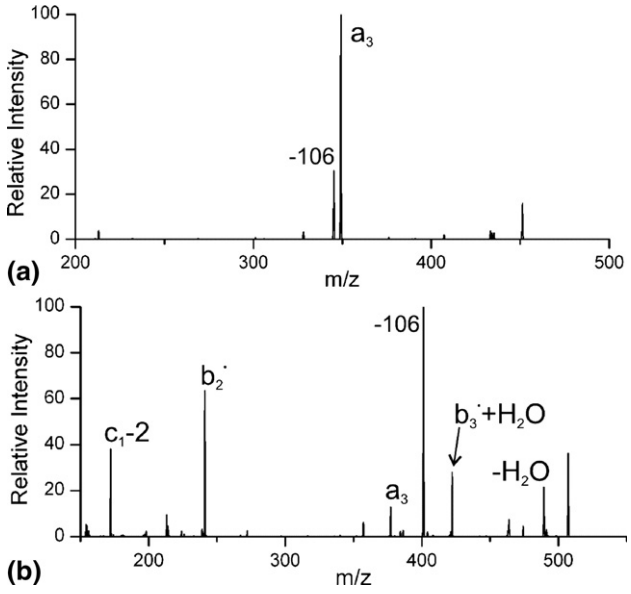

Figure 3. (**a**) CID of $[RGYG\cdot + H]^+$ yields backbone fragmentation at tyrosine (a_3) and loss of tyrosine side-chain. (**b**) The CID of $[RJYJ\cdot + H]^+$ is shown. Replacement of glycine with α-aminoisobutyric acid (J), which does not contain α-hydrogens, substantially diminishes selectivity.

N-terminal residue through a six-membered transition-state. For RGYALG, apparently scrambling to the C-terminal side is favored.

Radical Migration

As illustrated above and in previous work,[16, 35] radical migration can play an important role in the fragmentation of open-shell species. The CID spectrum of $[RGYG_{d2}\cdot + H]^+$ is shown in Figure 4a. The observation of singly deuterated a_3 ions unambiguously shows that a deuterium from the C-terminal glycine residue has migrated to the first three residues. Tandem MS can be used to pinpoint the residue where the deuterium has relocated. CID of the singly deuterated a_3 fragment (Figure 4b) produces a series of non- and singly deuterated b ions. Examination of d_1b_2 and b_2 reveals that the majority of the deuterium (75%) migrates to the tyrosine residue. The remaining deuterium (25%) is split between Arg1 and Gly2. Figure 4c shows the CID spectrum for $[RG_{d2}YG\cdot + H]^+$. All backbone fragments ($b_2^{\cdot}$, a_3) observed retain both deuteriums. In contrast to the CID of $[RGYG_{d2}\cdot + H]^+$, deuterium migration from Gly2 to Gly4 (either directly or indirectly) does not occur. The combined results suggest that radical migration not only occurs, but does so selectively. Since deuteration is unlikely to significantly affect conformational states, radical migration must be influenced by other factors.

There are two factors which contribute to barriers for radical migration in peptides. The first contribution results entirely from the nature of the donor and acceptor sites for the radical, or is simply a measure of the inherent "radical chemistry". The second contribution is introduced by conformational restraints which must be overcome to allow the donor and acceptor sites to interact. Conformational restraints may also affect radical transfer by preventing optimal alignment of the donor and acceptor groups. Conformational contributions to the barriers will vary in magnitude from zero to very high energies and are not easily calculated or generally applicable (i.e., they will be numerous and different for each peptide). For example, barriers have been calculated to be as high as 94.9 kJ/mol in 1,4 H-atom transfers due to bond angle strain, or as low as 50 kJ/mol in other amino acid systems [36–38]. On the other hand, barrier contributions due to radical chemistry alone can easily be calculated by examining radical transfer between two unconstrained molecules. Barriers

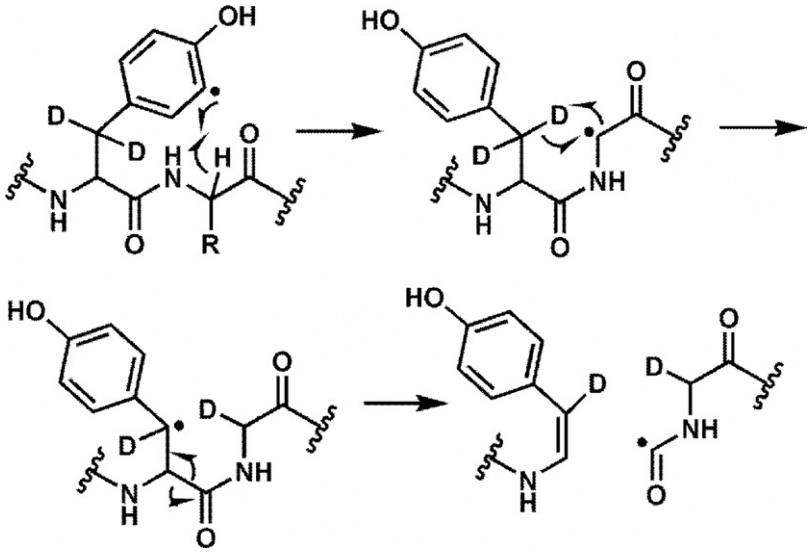

Scheme 3

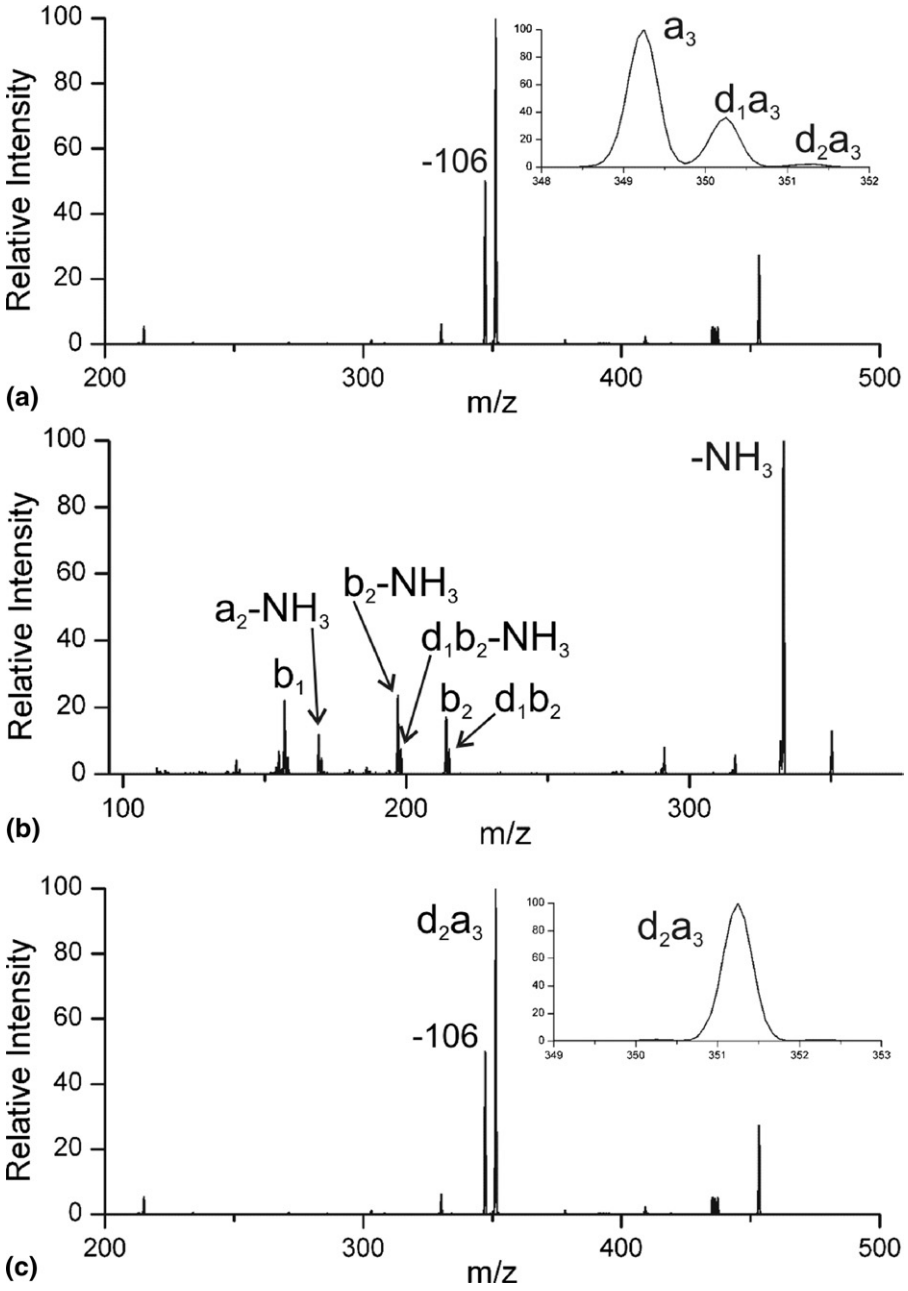

Figure 4. (**a**) CID of $[RGYG_{d2}\cdot + H]^+$ results in a deuterium transfer from the C-terminal glycine to the a_3 fragment. (**b**) CID of d_1a_3 from (**a**) indicates that 75% of the time, the scrambled deuterium resides on tyrosine. (**c**) CID of $[RG_{d2}YG\cdot + H]^+$ yields backbone fragmentation without extensive scrambling of the deuteriums on Gly2.

for abstraction by a tyrosyl radical from several relevant model molecules were calculated at the B3LYP/6-31++g(d,p) level of theory. Abstraction of the H_α of glycine by the tyrosyl radical has a calculated activation barrier of 8.8 kJ/mol. The optimized structures for the model tyrosyl radical - glycine complex (R1) and the transition-state (TS1) are shown in Scheme 4. Similarly, abstraction from benzylic and primary carbon sites also proceeds with minimal barriers, viz. 7.1 and 15.9 kJ/mol, respectively. These results agree with previous conformationally unconstrained calculations on related aromatic molecules [39]. Therefore, for a large variety of possible sites, the only substantial barriers to radical migration in peptides will originate from conformational constraints.

In contrast, a more substantial 73.2 kJ/mol barrier is calculated for hydrogen atom migration between glycyl radical and glycine, although this value is still lower than typical proton-driven dissociation barriers (120–140 kJ/mol) [40]. The optimized structures for glycyl radical–glycine complex (R2) and the transition-state (TS2) are shown in Scheme 4. The C_α–H bond of glycyl

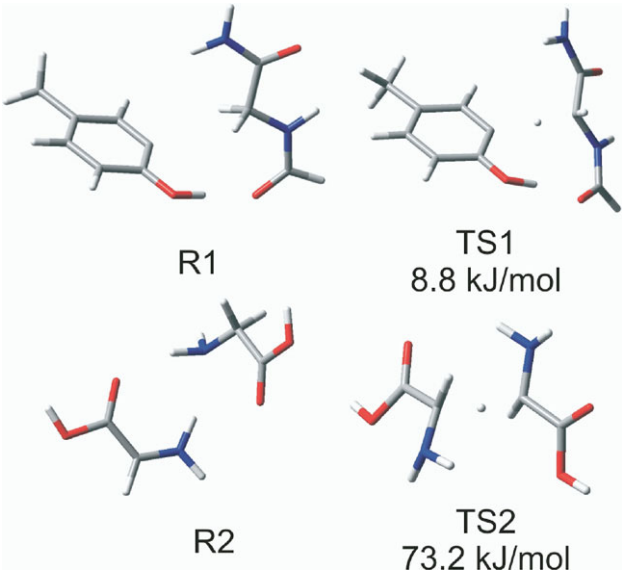

Scheme 4

radical must "bend" out-of-plane with respect to the adjacent amine and carboxylic acid groups to accommodate the incoming hydrogen atom from glycine. The energetic penalty associated with the loss of captodative stabilization in the transition-state complex gives rise to the observed barrier, which is an upper limit for glycyl radicals in peptides where stabilization may be considerably less. For example, glycyl radicals that are restricted from planarity due to secondary structure will have lower barriers to abstracting a hydrogen atom.

Recently, it has been reported that the B3LYP level of theory underestimates barrier heights for hydrogen atom abstraction and that MPW1K is a suitable alternative [38–42]. For the reactions shown, barrier heights calculated using the MPW1K/6-31+G(d,p)//B3LYP/6-31++(d,p) level of theory show a modest and systematic increase of ~8 kJ/mol compared to B3LYP. These barrier heights remain well below typical dissociation barriers and do not affect the main conclusions in this manuscript.

Theory therefore suggests modest to low barriers will exist for radical migration in peptides, with the dominant portion of the barrier frequently originating from conformational effects. The experimental results presented above indicate clearly that radical migration occurs before dissociation. Furthermore, radical directed dissociation dominates over proton initiated fragmentation in most cases. Taken together, these observations suggest that understanding radical migration is particularly important for predicting the ultimate fragmentation chemistry. The preference for particular backbone and side-chain fragmentations will be ultimately determined by the relevant kinetics controlling these dissociation pathways; however, since radical migration occurs below the fragmentation threshold, dissociation will be enhanced at sites to which the radicals preferentially migrate, (which correspond to thermodynamically favorable sites). Therefore backbone fragmentation at RGYALG, for example, occurs almost exclusively at tyrosine (the thermodynamically preferred destination), despite the presence of several other side chains with β carbons, which might offer similar kinetic constraints. Once the radical migrates to tyrosine, backbone dissociation is more favorable than subsequent radical migration to leucine, alanine or arginine, (which is both thermodynamically uphill and protected by kinetic barriers to fragmentation). We refer to the process of radical migration to thermodynamically favorable sites as radical funneling.

An interesting example is shown in Figure 5, where three related peptides with distinct radical initiation points yield essentially identical fragmentation. CID of $[RPPGYSPFR\cdot + H]^+$ yields a-type fragmentation at Tyr5 and at Phe8. The a_8 fragment is consistent with abstraction of the β hydrogen of phenylalanine, followed by β scission. Unlike fragmentation at tyrosine, dissociation at phenylalanine cannot occur by the rebound mechanism (although radical transfer to the adjacent α-carbon is possible). Furthermore, secondary backbone fragmentation at phenylalanine could occur by direct abstraction of the β hydrogen and does not

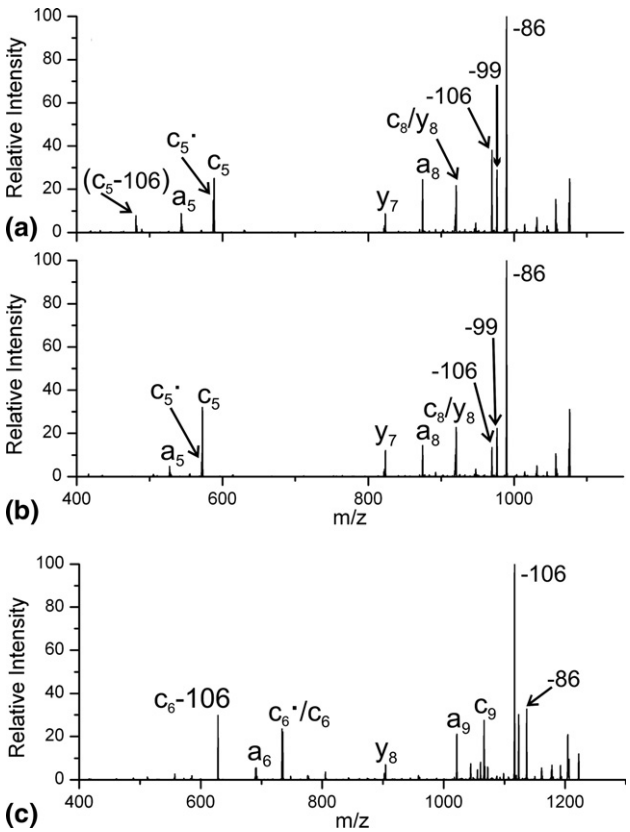

Figure 5. CID spectra of bradykinin analogs, (**a**) $[RPPGYSPFR\cdot + H]^+$, (**b**) $[RPPGFSPYR\cdot + H]^+$, and (**c**) $[YRPPGFSPFR\cdot + H]^+$ reveal similar backbone fragments despite different radical starting locations. The similarity suggests that the radical on each peptide scrambles to a similar distribution of radical isomers before dissociation.

strictly require an α-carbon radical intermediate. C-type fragments N-terminal to serine are also observed in Figure 5. This type of fragmentation has been documented previously and is produced from abstraction of the serine β hydrogen [14, 20].

CID of an analogous peptide where the positions of tyrosine and phenylalanine have been interchanged yields uncannily similar fragmentation. CID of $[RPPGFSPYR\cdot + H]^+$ is shown in Figure 5b. The only significant difference is the absence of the c_5-106 fragment. This is expected given that the c_5 in this peptide does not contain tyrosine and phenylalanine side-chain loss is not typically observed. All other backbone fragments are present in similar relative abundance, despite the difference in initial radical location. Figure 5c shows the CID spectrum of the radical peptide, YRPPGFSPFR, where the initial radical begins at the N-terminus. Surprisingly, backbone fragmentation still occurs at in similar relative abundances despite the quite different initial radical location.

The identical backbone fragmentation observed for all three bradykinin derivatives suggests that for a large peptide where many equivalent endpoints for radical migration may exist, the radical can migrate between these sites. Isomerization may occur through direct hydrogen atom abstraction between side chains, or by radical migration along the peptide backbone. Furthermore, migration may take place during the activation process. Regardless, the correspondence between the three spectra is consistent with rapid isomerization to similar radical intermediates, from which fragmentation occurs and yields a similar distribution of products. It is worth noting that CID of two of these radicals, $[RPPGYSPFR\cdot + H]^+$ and $[RPPGFSPYR\cdot + H]^+$, have been shown previously and yield qualitatively the same products [43]. Dissimilarities in ion abundances between our experiment and previous work likely arise from differences in preparation of the radical and ion trapping pressures.

Given inherent peptide structure, only radicals situated at the amide nitrogens, or at the α and β carbons may undergo β scission to cleave the backbone directly. The hydrogen-deuterium exchange experiments above indicate that the amide nitrogens are not favorable sites for radical migration. β-Scission from an α-carbon radical would necessitate cleavage of the resonance-stabilized amide bond and is therefore unfavorable. The amide BDE in the model compound, $CH_3C(O)–NH_2$, is 414 kJ/mol [22]. In contrast, the C_α–C(O) bond, which is cleaved by β scission from a β-centered radical, is expected to be easier to dissociate (BDE of $CH_3C(O)–CH_3$ is 354 kJ/mol). Additionally, a theoretical study of a closely related alkoxyl radical peptide predicts that β scission of the C_α–C(O) bond is essentially barrierless [44]. These results are consistent with preferential backbone fragmentation at residues with low C_β–H BDEs and the absence of backbone fragments from α-centered radicals. Thus, radical-induced fragmentation occurs only when a radical can access a thermodynamically favored site which is β to a weak bond, leading to a few preferred fragmentation channels. For large peptides, migration to sites with low C_β–H BDEs appears to be facile.

Conclusions

The mechanisms underlying backbone dissociation in radical peptides were studied using chemically modified derivatives and deuterium-labeling on model peptide scaffolds. We have shown that a radical positioned on the C_β of tyrosine is essential for producing a-type fragmentation at tyrosine. Movement of the radical from the initial site to the C_β is facilitated by a rebound mechanism between tyrosine and the adjacent amino acid. Failure of the radical to rebound and return to tyrosine yields side-chain losses and backbone fragmentation at other residues with low C_β–H BDEs. The results herein also indicate that the peptides studied are either structurally flexible or exist in highly heterogeneous ensembles, enabling the radical to sample multiple sites over multiple residues. We propose that radical migration preferentially yields backbone dissociation at sites with low C_β–H BDEs. Electronic energies, zero point vibrational energies, and coordinates for calculated structures can be found in the supplementary material, which can be found in the electronic version of this article.

Acknowledgments

The authors thank the National Science Foundation for funding (CHE-0747481).

Appendix A Supplementary Material

Supplementary material associated with this article may be found in the online version at doi:10.1016/j.jasms.2009.02.009.

References

1. Stubbe, J.; van der Donk, W. A. Protein Radicals in Enzyme Catalysis. *Chem. Rev.* **1998,** *98*, 705–762.
2. Zubarev, R. A.; Kelleher, N. L.; McLafferty, F. W. Electron capture dissociation of multiply charged protein cations: A nonergodic process. *J. Am. Chem. Soc.* **1998,** *120*, 3265–3266.
3. Syka, J. E. P.; Coon, J. J.; Schroeder, M. J.; Shabanowitz, J.; Hunt, D. F. Peptide and protein sequence analysis by electron transfer dissociation mass spectrometry. *Proc. Natl. Acad. Sci. U.S.A.* **2004,** *101*, 9528–9533.
4. Syrstad, E. A.; Turecek, F. Toward a general mechanism of electron capture dissociation. *J. Am. Soc. Mass Spectrom.* **2005,** *16*, 208–224.
5. Zubarev, R. A.; Kruger, N. A.; Fridriksson, E. K.; Lewis, M. A.; Horn, D. M.; Carpenter, B. K.; McLafferty, F. W. Electron capture dissociation of gaseous multiply charged proteins is favored at disulfide bonds and other sites of high hydrogen atom affinity. *J. Am. Chem. Soc.* **1999,** *121*, 2857–2862.
6. Zubarev, R. A.; Haselmann, K. F.; Budnik, B.; Kjeldsen, F.; Jensen, F. Towards an understanding of the mechanism of electron-capture dissociation: A historical perspective and modern ideas. *Eur. J. Mass Spectrom.* **2002,** *8*, 337–349.
7. Leymarie, N.; Costello, C. E.; O'Connor, P. B. Electron capture dissociation initiates a free radical reaction cascade. *J. Am. Chem. Soc.* **2003,** *125*, 8949–8958.
8. Jones, J. W.; Sasaki, T.; Goodlett, D. R.; Turecek, F. Electron capture in Spin-Trap Capped Peptides. An Experimental Example of Ergodic

Dissociation in Peptide Cation-Radicals. *J. Am. Soc. Mass Spectrom.* **2007,** *18*, 432–444.
9. Belyayev, M. A.; Cournoyer, J. J.; Lin, C.; O'Connor, P. B. The effect of radical trap moieties on electron capture dissociation spectra of substance P. *J. Am. Soc. Mass Spectrom.* **2006,** *17*, 1428–1436.
10. O'Connor, P. B.; Lin, C.; Cournoyer, J. J.; Pittman, J. L.; Belyayev, M.; Budnik, B. A. Long-lived electron capture dissociation product ions experience radical migration via hydrogen abstraction. *J. Am. Soc. Mass Spectrom.* **2006,** *17*, 576–585.
11. Prell, J. S.; O'Brien, J. T.; Holm, A. I. S.; Leib, R. D.; Donald, W. A.; Williams, E. R. Electron capture by a hydrated gaseous peptide: effects of water on fragmentation and molecular survival. *J. Am. Chem. Soc.* **2008,** *130*, 12680–12689.
12. Wee, S.; Mortimer, A.; Moran, D.; Wright, A.; Barlow, C. K.; O'Hair, R. A. J.; Radom, L.; Easton, C. J. Gas-phase regio-controlled generation of charged amino acid and peptide radicals. *Chem. Commun.* **2006,** *40*, 4233–4235.
13. Masterson, D. S.; Yin, H. Y.; Chacon, A.; Hachey, D. L.; Norris, J. L.; Porter, N. A. Lysine peroxycarbamates: Free radical-promoted peptide cleavage. *J. Am. Chem. Soc.* **2004,** *126*, 720–721.
14. Hodyss, R.; Cox, H. A.; Beauchamp, J. L. Bioconjugates for Tunable Peptide Sequencing: Free Radical Initiated Peptide Sequencing (FRIPS). *J. Am. Chem. Soc.* **2005,** *127*, 12436–12437.
15. Chu, I. K.; Rodriquez, C. F.; Lau, T. C.; Hopkinson, A. C.; Siu, K. W. M. Molecular Radical Cations of Oligopeptides. *J. Phys. Chem. B* **2000,** *104*, 3393–3397.
16. Wee, S.; O'Hair, R. A. J.; McFadyen, W. D. Comparing the gas phase fragmentation reactions of protonated and radical cations of the tripeptides GXR. *Int. J. Mass Spectrom.* **2004,** *234*, 101–122.
17. Laskin, J.; Yang, Z.; Chu, I. K. Energetics and Dynamics of Electron Transfer and Proton Transfer in Dissociation of $Metal^{III}$(salen)-Peptide Complexes in the Gas Phase. *J. Am. Chem. Soc.* **2008,** *130*, 3218–3230.
18. Thompson, M. S.; Cui, W. D.; Reilly, J. P. Fragmentation of singly charged peptide ions by photodissociation at l = 157 nm. *Angew. Chem. Int. Edit.* **2004,** *43*, 4791–4794.
19. Ly, T.; Julian, R. R. Residue-Specific Radical-Directed Dissociation of Whole Proteins in the Gas Phase. *J. Am. Chem. Soc.* **2008,** *130*, 351–358.
20. Sun, Q.; Nelson, H.; Ly, T.; Stoltz, B. M.; Julian, R. R. Side-chain chemistry mediates backbone fragmentation in hydrogen deficient peptide radicals. *J. Proteome Res.*, in press.
21. Diedrich, J. K.; Julian, R. R. Site-specific radical directed dissociation of peptides at phosphorylated residues. *J. Am. Chem. Soc.* **2008,** *130*, 12212–12213.
22. Blanksby, S. J.; Ellison, G. B. Bond dissociation energies of organic molecules. *Acc. Chem. Res.* **2003,** *36*, 255–263.
23. Rauk, A.; Yu, D.; Taylor, J.; Shustov, G. V.; Block, D. A.; Armstrong, D. A. Effects of structure on αC–H bond enthalpies of amino acid residues: relevance to H transfers in enzyme mechanisms and in protein oxidation. *Biochemistry* **1999,** *38*, 9089–9096.
24. Kavita, K.; Das, P. K. Photodissociation of C_6H_5I, C_6F_5I, and related iodides in the ultraviolet. *J. Chem. Phys.* **2002,** *117*, 2038–2044.
25. Paquet, A. Introduction of 9-fluorenylmethyloxycarbonyl, trichloroethoxycarbonyl, and benzyloxycarbonyl amine protecting groups into O-unprotected hydroxyamino acids using succinimidyl carbonates. *Can. J. Chem.* **1982,** *60*, 976–980.
26. Carpino, L. A.; Han, G. Y. The 9-fluorenylmethyloxycarbonyl amino-protecting group. *J. Org. Chem.* **1972,** *37*, 3404–3408.
27. Chan, W. C.; White, P. D., Eds. Fmoc Solid Phase Peptide Synthesis: A Practical Approach. Oxford University Press: New York, NY, 2004.
28. Kim, T. Y.; Thompson, M. S.; Reilly, J. P. Peptide photodissociation at 157 nm in a linear ion trap mass spectrometer. *Rapid Commun. Mass Spectrom.* **2005,** *19*, 1657–1665.
29. Gronert, S. Estimation of effective ion temperatures in a quadrupole ion trap. *J. Am. Soc. Mass Spectrom.* **1998,** *9*, 845–848.
30. Peng, C. Y.; Schlegel, H. B. Combining synchronous transit and quasi-Newton methods to find transition states. *Israel J. Chem.* **1993,** *33*, 449–454.
31. Nielsen, M. L.; Budnik, B. A.; Haselmann, K. F.; Olsen, J. V.; Zubarev, R. A. Intramolecular hydrogen atom transfer in hydrogen-deficient polypeptide radical cations. *Chem. Phys. Lett.* **2000,** *330(5/6)*, 558–562.
32. Kenny, P. T. M.; Nomoto, K.; Orlando, R. Fragmentation Studies of Peptides - the Formation of Y-Ions. *Rapid Commun. Mass Spectrom.* **1992,** *6(2)*, 95–97.
33. Harrison, A. G.; Yalcin, T. Proton mobility in protonated amino acids and peptides. *Int. J. Mass Spectrom. Ion Processes* **1997,** *165*, 339–347.
34. Dunlop, J. R.; Tully, F. P. A kinetic study of OH radical reactions with methane and perdeuterated methane. *J. Phys. Chem.* **1993,** *97*, 11148–11150.
35. Laskin, J.; Futrell, J. H.; Chu, I. K. Is dissociation of peptide radical cations an ergodic process? *J. Am. Chem. Soc.* **2007,** *129*, 9598–9599.
36. Moran, D.; Jacob, R.; Wood, G. P. F.; Coote, M. L.; Davies, M. J.; O'Hair, R. A. J.; Easton, C. J.; Radom, L. Rearrangements in model peptide-type radicals via intramolecular hydrogen-atom transfer. *Helv. Chim. Acta* **2006,** *89*, 2254–2272.
37. Fung, W. M. E.; Chan, T. W. D. Experimental and theoretical investigations of the loss of amino acid side chains in electron capture dissociation of model peptides. *J. Am. Soc. Mass Spectrom.* **2005,** *16*, 1523–1535.
38. Panja, S.; Nielsen, S. B.; Hvelplund, P.; Turecek, F. Inverse hydrogen migration in arginine-containing peptide ions upon electron transfer. *J. Am. Soc. Mass Spectrom.* **2008,** *19*, 1726–1742.
39. Jing, L.; Nash, J. J.; Kenttamaa, H. I. Correlation of hydrogen-atom abstraction reaction efficiencies for aryl radicals with their vertical electron affinities and vertical ionization energies of the hydrogen-atom donors. *J. Am. Chem. Soc.* **2008,** *130*, 17697–17709.
40. Paizs, B.; Suhai, S. Towards understanding the tandem mass spectra of protonated oligopeptides. 1: Mechanism of amide bond cleavage. *J. Am. Soc. Mass Spectrom.* **2004,** *15*, 103–113.
41. Lynch, B. J.; Fast, P. L.; Harris, M.; Truhlar, D. G. Adiabatic connection for kinetics. *J. Phys. Chem. A* **2000,** *104*, 4811–4815.
42. Lingwood, M.; Hammond, J. R.; Hrovat, D. A.; Mayer, J. M.; Borden, J. MPW1K performs much better than B3LYP in DFT calculations on reactions that proceed by proton-coupled electron transfer (PCET). *Chem. Theory Comput.* **2006,** *2*, 740–745.
43. Laskin, J.; Yang, Z.; Lam, C.; Chu, I. K. Charge-remote fragmentation of odd-electron peptide ions. *Anal. Chem.* **2007,** *79*, 6607–6614.
44. Wood, G. P. F.; Easton, C. J.; Rauk, A.; Davies, M. J.; Radom, L. Effect of side chains on competing pathways for β-scission reactions of peptide-backbone alkoxyl radicals. *J. Phys. Chem. A* **2006,** *110*, 10316–10323.